

Chapter 4

Forced Convection Around Obstacles

4.1. Description of the flow

This chapter is devoted to heat transfer on bodies immersed in a stream. We consider a solid characterized by the length scale L placed in a stream characterized by the reference velocity U , which is generally the velocity far upstream from the obstacle (several times the length L in practice). If the solid is heated to a temperature T_∞ different from that of the fluid, heat transfer occurs in the vicinity of the solid surface and in the downstream wake. The thermal field depends strongly on the flow field, which is characterized by the Reynolds number $Re = UL/\nu$.

We first distinguish the flows at $Re \ll 1$ and $Re \gg 1$. The first type of flow is present in limited domains of application (sedimentation, thermo-anemometry). These creeping flows are governed by viscous effects.

Flows of the second type ($Re \gg 1$) are more often encountered in practical applications. These flows are characterized by thin velocity and thermal boundary layers in the upstream part of the obstacle. A particular streamline ends at a stagnation point A located in front of the obstacle. Boundary layers originate in the stagnation region and then grow in the downstream direction up to the trailing edge for streamlined bodies (Figure 4.1). A velocity wake (velocity defect) and a thermal wake (temperature excess when the solid is heated) develop behind the obstacle. The wake region follows the development of the boundary layers when the obstacle is well profiled.

When the obstacle is not well profiled (bluff body), the flow separates at some distance downstream from the stagnation point, where the pressure would have

tended to increase in the absence of separation. The circular cylinder is a typical example of such obstacles (Figure 4.2). For bluff bodies, the wake is much broader than for streamlined airfoils.

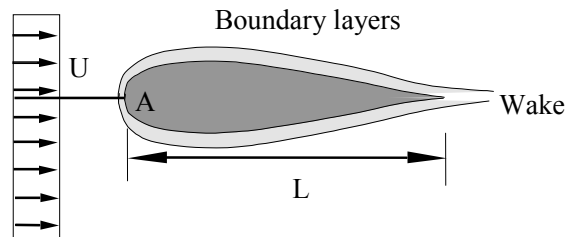


Figure 4.1. Flow near a streamlined body. $Re \gg 1$

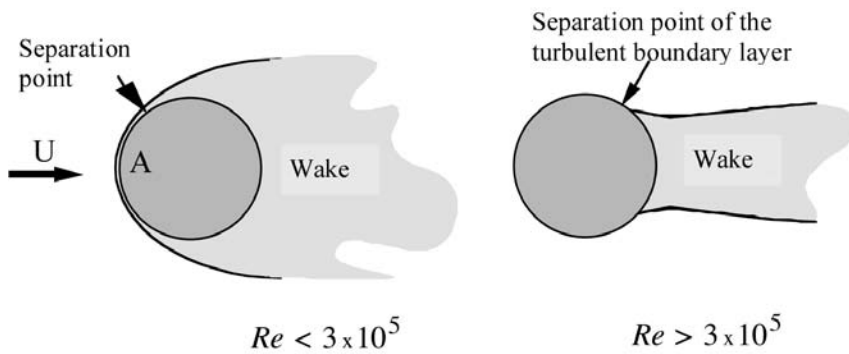


Figure 4.2. Flow near a circular cylinder. $Re \gg 1$

For a circular cylinder of diameter D , the Reynolds number is defined by $Re = UD/\nu$. When $Re < 3 \times 10^5$, the separation point is located at an angle $\phi \sim 80^\circ$, counted from the stagnation point A.

When $Re > 3 \times 10^5$, the boundary layer becomes turbulent in the upstream part of the cylinder and the separation point moves downstream, say at an angle $\phi \sim 120^\circ$.

The case of a circular cylinder has been investigated in many studies. Several flow regimes may be distinguished in the range $Re > 1$. Alternate vortices are generated at the rear side of the cylinder for Re higher than about 50 (Karman vortex street). The complexity of the flow field topology increases in the wake along with the Reynolds number.

4.2. Local heat-transfer coefficient for a circular cylinder

We consider a circular cylinder of radius R (diameter D) at uniform temperature T_w immersed in a stream of uniform velocity at temperature T_∞ (Figure 4.3). A current point M of the cylinder surface is determined by its curvilinear abscissa x ($= R\phi$), counted from the stagnation point A . The local heat-transfer coefficient $h(x)$ is defined with the local heat flux $q''(x)$ exchanged between the cylinder and the fluid as

$$q''(x) = h(x)(T_w - T_\infty) \quad [4.1]$$

The local heat-transfer coefficient depends on the position of M , the Reynolds and the Prandtl numbers. The local Nusselt number is proportional to $h(x)$:

$$Nu = \frac{h(x)D}{k} \quad [4.2]$$

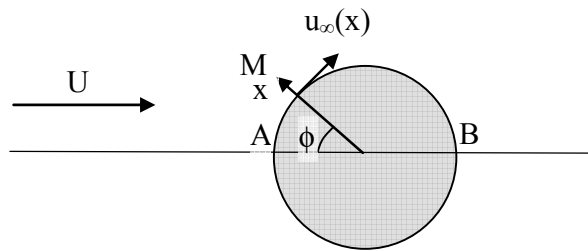


Figure 4.3. Circular cylinder in a uniform stream. Definitions

In the upstream region close to the cylinder, the flow is characterized by laminar boundary layers so that $Nu \approx \sqrt{Re}$, or equivalently Nu/\sqrt{Re} , is independent of Re . The distribution of Nu on the cylinder surface is shown in Figure 4.4 for air flow ($Pr = 0.7$). Experimental results (symbols in Figure 4.4) show that $Nu/\sqrt{Re} \approx 1$ at the front stagnation point A ($\phi = 0$). The heat-transfer coefficient decreases in the downstream direction, which corresponds to boundary layer thickening. Contrary to the upstream part of the cylinder, the ratio Nu/\sqrt{Re} depends on Re in the downstream part of the flow, where the wake configuration depends on Re . Figure 4.5 shows experimental results for the heat-transfer coefficient at the downstream stagnation point B on the rear side of the cylinder ($\phi = \pi$). It is worth noting that Nu/\sqrt{Re} is smaller at point B than at point A for $Re < 10^4$.

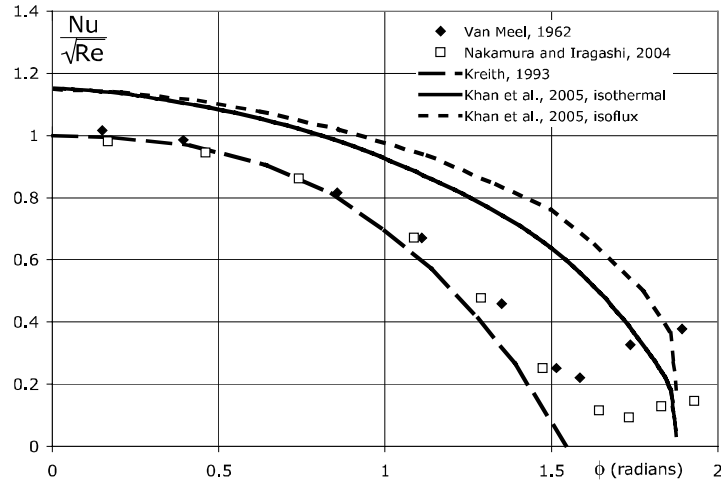


Figure 4.4. Nusselt number on the upstream part of a cylinder in air; adapted from [KHA 05]

For high Reynolds number flows it is possible to calculate the heat-transfer coefficient $h(x)$ in the laminar boundary layer that develops on the upstream side of the cylinder. The result depends on the external velocity law $u_\infty(x)$ that is chosen for the calculation (Figure 4.3). Potential flow theory gives the velocity distribution outside the boundary layer:

$$u_\infty(x)/U = 2 \sin(x/R) \quad [4.3]$$

However, separation has a significant effect on the flow on the upstream side of the cylinder and the following law is closer than [4.3] to the actual velocity distribution near the cylinder surface:

$$u_\infty(x)/U = 3.631(x/d) - 3.275(x/d)^2 - 0.168(x/d)^5 \quad [4.4]$$

Several approaches have been proposed for calculation of $h(x)$. A review may be found in [SPA 62]. The different approaches may be classified according to the principles that they used:

- local similarity;
- integral method using two equations;
- method using one equation, which combines the integral energy equation and similarity solutions to boundary layer equations [SMI 58].

Figure 4.4 shows the results obtained by [KHA 05] with the integral method and the external velocity law [4.3]. This calculation slightly overpredicts ($\approx 15\%$) the Nusselt number when compared to experimental results. This discrepancy may be due to the method accuracy or to the velocity law chosen by the authors.

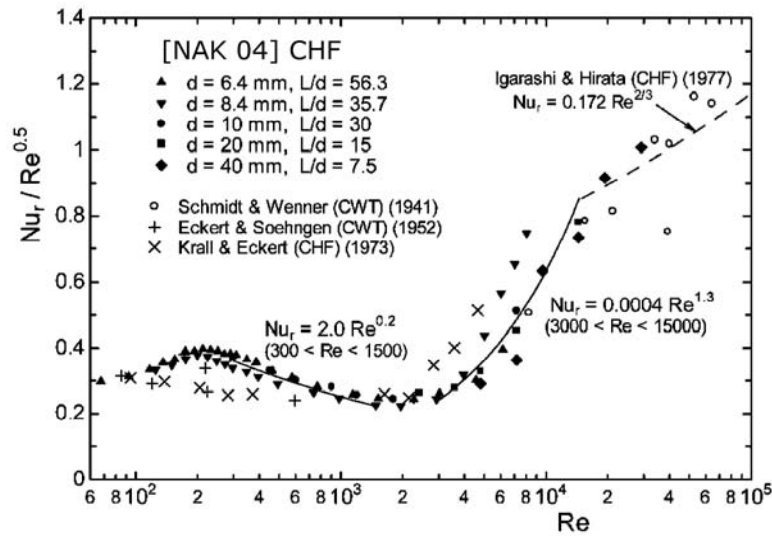


Figure 4.5. Nusselt number at the rear stagnation point of a cylinder in air [NAK 04]. CHF: constant heat flux, CWT: constant wall temperature. Reprinted from *Int. J. of Heat and Mass Transfer*, Vol. 47, NAKAMURA H., IGARASHI T., Variation of Nusselt number with flow regimes behind a circular cylinder for Reynolds numbers from 70 to 30,000, pages 5169-5173, copyright 2004, with permission from Elsevier

4.3. Average heat-transfer coefficient for a circular cylinder

The overall rate of heat exchanged by transverse unit, $q' = q/L_z$, between the cylinder and the flow is represented by the average heat-transfer coefficient \bar{h} ¹

$$q/\pi DL_z = \bar{h}(T_w - T_\infty) \quad [4.5]$$

1. The average heat-transfer coefficient \bar{h} is defined here by a spatial average and should not be confused with the time average used in Chapter 7 for a time-varying quantity in turbulent flows.

or in dimensionless form

$$\overline{Nu} = \frac{\overline{h}D}{k} = \frac{q/\pi DL_z}{k(T_w - T_\infty)/D} \quad [4.6]$$

\overline{Nu} depends on Re and Pr . Many correlations are available in the literature. For example, Churchill and Bernstein [CHU 77a] recommend:

$$\overline{Nu} = 0.3 + \frac{0.62Re^{1/2}Pr^{1/3}}{\left[1 + (0.4/Pr)^{2/3}\right]^{1/4}} \left[1 + \left(\frac{Re}{282\,000}\right)^{5/8}\right]^{-4/5} \quad [4.7]$$

for $0.2 < Pe = Re Pr$.

\overline{Nu} , Re , Pr are calculated with the fluid physical properties at the film temperature $T_f = (T_w + T_\infty)/2$. For uniform wall heat flux, equation [4.7] may be used with the temperature averaged on the cylinder perimeter. [BEJ 95] indicates that equation [4.7] underestimates the Nusselt number by up to 20% when compared to experimental results in the range $7 \times 10^4 < Re < 4 \times 10^5$.

The law of Collis and Williams [COL 59] may be applied to low Reynolds number air flows and consequently to thermo-anemometry applications

$$\overline{Nu} = (A + BRe^n) \left(T_\infty/T_f\right)^a \quad [4.8]$$

where the coefficients n , A , B and a are given in Table 4.1.

| | $0.02 < Re < 44$ | $44 < Re < 140$ |
|-----|------------------|-----------------|
| n | 0.45 | 0.51 |
| A | 0.24 | 0 |
| B | 0.56 | 0.48 |
| a | -0.17 | -0.17 |

Table 4.1. Coefficients of the Collis and Williams law [COL 59]

The fluid physical properties are evaluated at $T_f = (T_w + T_\infty)/2$.

Nakamura and Igarashi [NAK 04] give the results in Figure 4.6.

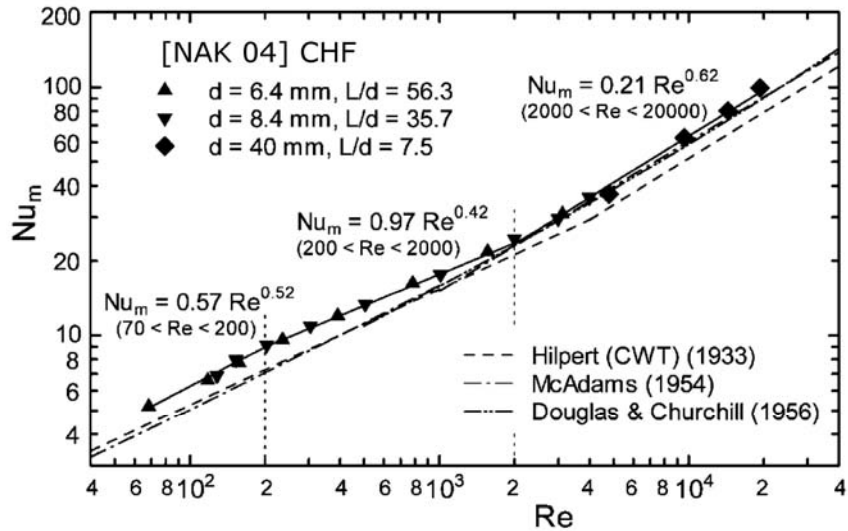


Figure 4.6. Overall Nusselt number for a circular cylinder [NAK 04]. Reprinted from *Int. J. of Heat and Mass Transfer*, Vol 47, NAKAMURA H., IGARASHI T., Variation of Nusselt number with flow regimes behind a circular cylinder for Reynolds numbers from 70 to 30,000, pages 5169–5173, copyright 2004, with permission from Elsevier

4.4. Other obstacles

Heat transfer between a uniform stream and a sphere is represented by [WHI 91]

$$\overline{Nu} = 2 + (0.4Re^{1/2} + 0.06Re^{2/3})Pr^{0.4}(\mu_f/\mu_w)^{1/4} \quad [4.9]$$

for $0.71 < Pr < 380$, $3.5 < Re < 7.6 \times 10^4$, $1 < \mu_f/\mu_w < 3.2$.

A review of several papers on this topic and the following correlation may be found in [MEL 05]

$$\overline{Nu} = 2 + 0.47Re^{1/2}Pr^{0.36} \quad [4.10]$$

for $3 \times 10^{-3} < Pr < 10$, $10^2 < Re < 5 \times 10^4$.

4.5. Heat transfer for a rectangular plate in cross-flow

4.5.1. Description of the problem

A heated rectangular plate (height d , span length L_z , negligible thickness) is placed in a uniform cross-flow (Figure 4.7). We consider the rate of heat exchanged between the rear side of the plate and the fluid. The lateral sides of the plate are assumed to be perfectly insulated.

In order to determine the law governing heat transfer between the plate and the fluid, a series of experimental tests is performed in a flow of water at different velocities. The plate is maintained at the constant temperature $T_w = 70^\circ\text{C}$ by electrical heating. A film that is electrically heated covers the rear side of the plate. Measurements give the electric power q necessary to keep the film at the constant temperature $T_w = 70^\circ\text{C}$ when the temperature of water is 20°C .

The dimensions of the plate are $d = 2$ cm, $L_z = 20$ cm.

The physical properties of water are:

- kinematic viscosity $\nu = 6 \times 10^{-7} \text{ m}^2 \text{ s}^{-1}$
- thermal conductivity $k = 0.63 \text{ W m}^{-1} \text{ K}^{-1}$
- specific heat at constant pressure $C_p = 4.18 \cdot 10^3 \text{ J kg}^{-1} \text{ K}^{-1}$

Using the test results shown in Table 4.2, propose a correlation for heat transfer between the plate and the flow.

4.5.2. Solution

Since the plate is insulated at its lateral sides and uniformly heated in the spanwise direction, we assume that the temperature field is two-dimensional, both in the plate and in the fluid domains. The span length L_z therefore neither plays any role in the flow nor in the global heat-transfer coefficient between the plate and the flow.

This statement would be incorrect if heat losses take place at the lateral sides of the plate. In this case, transverse conduction would occur along the plate so that the temperature field would be three-dimensional.

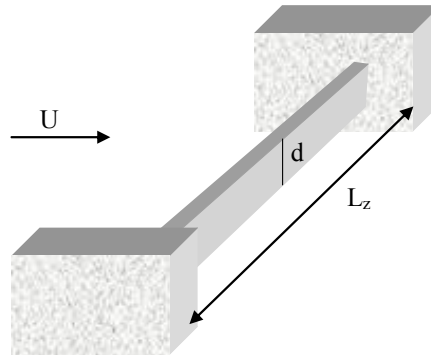


Figure 4.7. Rectangular plate placed in a uniform cross-flow

| | | | | | |
|-------------|-----|-----|------|------|------|
| U (m/s) | 0.2 | 0.4 | 0.8 | 1.2 | 1.6 |
| q (watts) | 485 | 805 | 1150 | 1650 | 2250 |

Table 4.2. Electrical power supplied to the rear film against velocity

With these assumptions, the flow is only characterized by the Reynolds number $Re = Ud/\nu$ and heat transfer by the global Nusselt number $\overline{Nu} = \frac{\overline{h}d}{k}$ with $q_{conv}/dL_z = \overline{h}(T_w - T_\infty)$.

If heat losses are ignored (transverse conductive flux, radiation), the convective heat transfer rate at the rear side of the plate balances the electrical power due to the Joule effect in the film, $q_{conv} = q$. As the working fluid is unchanged during the experiments, the Prandtl number is kept constant. The heat transfer law is then of the form $\overline{Nu} = f(Re)$. The two dimensionless numbers are given in Table 4.3. The results are plotted using logarithmic scales because a heat transfer correlation of the power-law type, like [4.7], is expected.

| | | | | | |
|-------------------------------------|-------------------|--------------------|--------------------|-----------------|--------------------|
| U (m s ⁻¹) | 0.2 | 0.4 | 0.8 | 1.2 | 1.6 |
| Re | 3.3×10^3 | 6.67×10^3 | 1.33×10^3 | 2×10^4 | 2.67×10^4 |
| q (watts) | 485 | 805 | 1150 | 1650 | 2250 |
| \overline{h} (W m ⁻²) | 4850 | 8050 | 11500 | 16500 | 22500 |
| \overline{Nu} | 77 | 127.8 | 182.5 | 261.9 | 357.1 |

Table 4.3. Interpretation of the results by using dimensionless variables

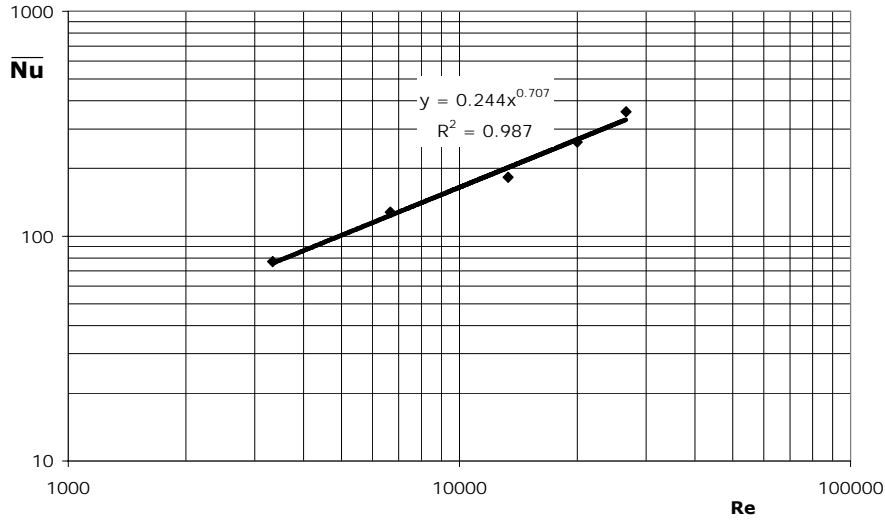


Figure 4.8. Representation of the results with dimensionless variables (logarithmic scales)

The experimental points are roughly aligned in this logarithmic-scale plot in Figure 4.8. We deduce the empirical heat transfer correlation for air:

$$\overline{Nu} = 0.24Re^{0.7} \quad [4.11]$$

Using their experimental results obtained with uniform flux heating in air, [RAM 02] propose the following correlation for the rear side of a plate of aspect ratio $L_z/d = 6$:

$$\text{For } 5.6 \times 10^3 < Re < 3.85 \times 10^4 \quad \overline{Nu} = 0.16Re^{0.72}$$

4.6. Heat transfer in a stagnation plane flow. Uniform temperature heating

4.6.1. Description of the problem

A two-dimensional body is placed in a stream of air (temperature far from the obstacle T_∞). We consider heat transfer near the upstream stagnation line, where the flow is assumed to be laminar. The problem is restricted to the case of a plane plate of length $2L_x$ perpendicular to the stream (Figure 4.9). The similarity solutions to the Falkner-Skan equations are used to determine the flow (Figure 3.2 for the general case). Velocity and shear stress profiles are shown in dimensionless variables in Figure 3.3 and in Table 3.1 as a function of the parameter m .

The physical properties of air are:

- density $\rho = 1.29 \text{ kg m}^{-3}$
- kinematic viscosity $\nu = 13 \times 10^{-6} \text{ m}^2 \text{ s}^{-1}$
- thermal conductivity $k = 0.024 \text{ W m}^{-1} \text{ K}^{-1}$
- Prandtl number $Pr = 0.72$

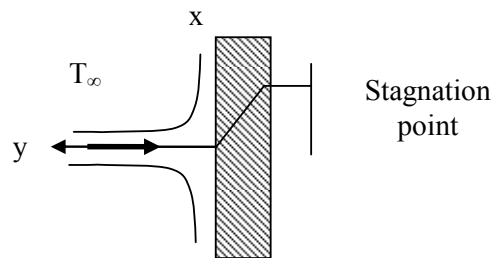


Figure 4.9. Flow perpendicular to a plane plate

4.6.2. Guidelines

Give the external velocity law for the boundary layer that develops on the plate. It is assumed that the velocity scale is fixed at some point of the plate, for example at its edges in x -direction. In other words, the coefficient K of the external velocity law is assumed to be known. Give the order of magnitude δ of the boundary layer thickness. Calculate this thickness by using Figure 3.3. Calculate the shear stress τ exerted by the flow on the wall as a function of x using Table 3.1.

The wall is heated at uniform temperature T_w . Using the similarity solutions to the energy equation in the forced laminar regime, express the local Nusselt number Nu_x as a function of the local Reynolds number and the Prandtl number. Express the heat-transfer coefficient as a function of the parameters that define the problem conditions.

Numerically calculate the thickness δ for $K = 1000 \text{ s}^{-1}$ and the shear stress for $x = 5 \text{ cm}$. Calculate the local heat flux exchanged between the fluid and the plate for these values of x , K and $T_w = 5 \text{ K}$, $T_\infty = -5 \text{ K}$ (the plate is heated to avoid icing on the wall). Calculate the overall heat transfer rate exchanged by the plate of length $2L_x = 10 \text{ cm}$ and span length $L_z = 50 \text{ cm}$.

4.6.3. Solution

4.6.3.1. Flow field

For a two-dimensional stagnation-point flow on a flat plate, the angle of the reference wedge is $\beta\pi = \pi$ (Figure 3.2), from which it follows that $\beta=1$ and $m=1$. The external velocity law is $u_\infty(x) = Kx$ for the boundary layer that develops on the plate.

For a laminar boundary layer in forced convection, scale analysis gives the order of magnitude $\delta/x \approx 1/\sqrt{Re_x}$ with $Re_x = u_\infty(x)x/\nu$ (equation [3.5]). Replacing $u_\infty(x)$ with the above expression in Re_x , we find that the boundary layer thickness is constant with x . Let us denote:

$$\delta_1 = \sqrt{\frac{\nu}{K}} \quad [4.12]$$

Figure 3.3 shows that the thickness may be estimated more precisely by $\eta \approx 2.5$, which gives the thickness $\delta_2 \approx 2.5\delta_1$.

The wall shear stress is related to the similarity function F by:

$$\tau_0(x) = \mu \left. \frac{\partial u(x, y)}{\partial y} \right|_{y=0} = \mu \frac{u_\infty(x)}{\delta_1} F''(0) \quad [4.13]$$

Table 3.1 gives $F''(0) = 1.232$. Thus, the wall shear stress varies linearly with x as:

$$\tau_0 = 1.232\mu \sqrt{\frac{K^3}{\nu}} x \quad [4.14]$$

4.6.3.2. Heat transfer

A favorable pressure gradient leads to an increase in the Nusselt number when compared to a flow with zero pressure gradient. In the case of uniform temperature heating, Table 3.3 gives the ratio:

$$\frac{Nu(m=1, Pr=0, 7)}{Nu(m=0, Pr=0, 7)} \approx 1.7$$

Using the heat transfer law for a plane plate (equation [3.24]), the local Nusselt number is obtained as:

$$Nu_x \approx 1.7 \times 0.332 Re_x^{1/2} Pr^{1/3} \approx 0.564 Re_x^{1/2} Pr^{1/3} \quad [4.15]$$

The heat-transfer coefficient is therefore constant with x :

$$h = 0.564 k \sqrt{\frac{K}{\nu}} Pr^{1/3} \quad [4.16]$$

With the data given above, we calculate for $x = 5$ cm:

$$\delta_2 = 0.28 \text{ mm}, \quad \tau_0 = 9.1 \text{ Nm}^{-2}, \quad h = 106.5 \text{ Wm}^{-2}\text{K}^{-1}$$

The local heat flux is $q'' = h(T_\infty - T_w) = 1065 \text{ Wm}^{-2}$ and the total heat transfer rate exchanged between the fluid and the plate is $q = q'' 2L_x L_z = 53 \text{ W}$.

4.7. Heat transfer in a stagnation plane flow. Step-wise heating at uniform flux

4.7.1. Description of the problem

We again consider the problem in section 4.6 with, however, two important differences. The plate heating is now started at a location downstream from the stagnation point (Figure 4.10). Moreover, the plate is heated at uniform flux instead of uniform temperature. The plate is unheated on the length x_0 so that a thermal boundary layer develops beyond this starting length and is therefore embedded in the velocity boundary layer that starts at the leading edge of the plate. The plate is heated at uniform flux q''_0 for $x \geq x_0$. The wall temperature is then T_∞ for $x < x_0$ and increases further downstream.

The unknown wall temperature is denoted $T_w(x)$ in the heated region. Let us denote $\Theta(x) = T_w(x) - T_\infty$.

We plan to determine the heat transfer law between the wall and the fluid for $x \geq x_0$.

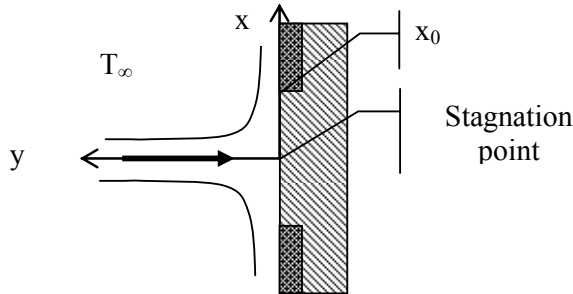


Figure 4.10. Step-wise heating at uniform flux

4.7.2. Guidelines

The problem is restricted to the initial region of the thermal boundary layer. Propose a velocity profile $u(x,y)$ inside the thermal boundary layer by using Figure 3.3 and replace the actual velocity profile near the wall by its tangent at the origin.

Use the integral energy equation applied to a boundary layer flow. Assume that the heat flux q_0'' is independent of x and determine the rate of enthalpy convected through a section perpendicular to the wall as a function of x .

It is suggested that the following polynomial be used to represent the temperature profile in the thermal boundary layer of thickness $\delta_T(x)$

$$\frac{T(x, y) - T_\infty}{T_w(x) - T_\infty} = \theta(\zeta) = 1 - \left(\frac{3}{2} \zeta - \frac{1}{2} \zeta^3 \right) \tag{4.17}$$

with $\zeta = y/\delta_T(x)$, $0 \leq \zeta \leq 1$.

Determine a relation between $\Theta(x)$ and $\delta_T(x)$ (take the boundary condition in $x = x_0$ into account).

Use the profile given by equation [4.17] in the relation between the heat flux and the temperature gradient at the wall and find a second equation between $\Theta(x)$ and $\delta_T(x)$.

Combine these equations to calculate $\Theta(x)$ and $\delta_T(x)$. Determine the heat transfer law giving the local Nusselt number Nu_x as a function of Re_x and the ratio x_0/x . Verify that when $x_0 = 0$, the heat transfer law is close to that issuing from the similarity solution.

4.7.3. Solution

4.7.3.1. Modeling the velocity profile

Replacing the actual velocity profile near the wall by its tangent at the origin and using [4.13], we obtain

$$\frac{u(x, y)}{u_\infty(x)} = F_0'' \frac{y}{\delta_1} \quad [4.18]$$

with $F_0'' = 1.232$ or

$$u(x, y) = \lambda xy \quad [4.19]$$

with $\lambda = 1.232 \frac{K}{\delta_1} = 1.232 \sqrt{\frac{K^3}{\nu}}$.

4.7.3.2. Integral energy equation

The integral energy equation reads (see Chapter 3, equation [3.33]):

$$\frac{d}{dx} \int_0^\infty \rho C_p u(x, y) [T(x, y) - T_\infty] dy = q''(x) = -k \left(\frac{\partial T}{\partial y} \right)_0 \quad [4.20]$$

In the conditions of the present problem, the heat flux is independent of x ($q''(x) = q_0''$), so that the above equation may be integrated as:

$$\int_0^\infty \rho C_p u(x, y) [T(x, y) - T_\infty] dy = q_0'' x + C_1 \quad [4.21]$$

The expressions chosen for the velocity and temperature profiles are then reported in [4.21]:

$$\int_0^\infty \rho C_p \lambda xy \Theta(x) \theta(\zeta) dy = q_0'' x + C_1$$

We eliminate y in favor of ζ by using $y = \delta_T(x) \zeta$ and we obtain a first equation satisfied by the unknown functions $\Theta(x)$ and $\delta_T(x)$,

$$A \lambda \rho C_p x \delta_T(x)^2 \Theta(x) = q_0'' x + C_1 \quad [4.22]$$

with $A = \int_0^1 \theta(\zeta) \zeta d\zeta$. The modeled temperature profile [4.17] gives $A = 1/10$.

4.7.3.3. *Heat flux*

The modeled temperature profile [4.17] is also used in the expression of the heat flux as:

$$q_0'' = -k \left(\frac{\partial T}{\partial y} \right)_0 = -k \frac{\Theta(x)}{\delta_T(x)} \theta'(0)$$

The chosen profile gives $\theta'(0) = -\frac{3}{2}$.

The second equation satisfied by the unknowns of the problem is therefore:

$$-\frac{3}{2} k \frac{\Theta(x)}{\delta_T(x)} = q_0'' \quad [4.23]$$

4.7.3.4. *Heat transfer law*

The solution of the system of equations [4.22] and [4.23] gives for $x \geq x_0$ the distribution of:

– the boundary layer thickness:

$$\delta_T(x) = \left[12.2 \alpha \sqrt{\frac{\nu}{K^3}} \left(1 - \frac{x_0}{x} \right) \right]^{1/3} \quad [4.24]$$

– the wall temperature:

$$\Theta(x) = \frac{2}{3} \frac{q_0''}{k} \left[12.2 \alpha \sqrt{\frac{\nu}{K^3}} \left(1 - \frac{x_0}{x} \right) \right]^{1/3} \quad [4.25]$$

– and the Nusselt number:

$$Nu(x) = \frac{q_0''}{k \frac{\Theta(x)}{x}} = 0.65 x \left[\alpha \sqrt{\frac{\nu}{K^3}} \left(1 - \frac{x_0}{x} \right) \right]^{-1/3} \quad [4.26]$$

– or, as a function of $Re_x = \frac{u_\infty(x)x}{\nu} = \frac{Kx^2}{\nu}$:

$$Nu(x) = \frac{q_0''}{k \frac{\Theta(x)}{x}} = 0.65 \frac{Re_x^{1/2} Pr^{1/3}}{\left(1 - \frac{x_0}{x}\right)^{1/3}} \quad [4.27]$$

For $x_0 = 0$, the heat transfer law becomes:

$$Nu(x) = 0.65 Re_x^{1/2} Pr^{1/3}$$

A similarity solution to the energy equation is available in this particular case. Table 3.3 gives the ratio $Nu_x(m)/Nu_x(m=0)$ for uniform temperature heating. When the fluid is air ($Pr = 0.72$), this ratio has the value 1.696. $Nu_x(m=0)$ is given by equation [3.23]. The result must be further corrected for uniform flux heating (equation [3.26]). Thus, the Nusselt number issuing from the similarity solution is:

$$Nu(x) = 0.332 \times 1.696 \times 1.31 Re_x^{1/2} Pr^{1/3} = 0.74 Re_x^{1/2} Pr^{1/3}$$

The integral method underestimates the heat-transfer coefficient by 12%.

4.8. Temperature measurements by cold-wire

4.8.1. Description of the problem

Temperature measurements in a turbulent flow are often performed with the cold-wire method (see, for example, [BRU 95]).

The measurements are performed with an electric wire with a very small diameter d , length l , and electric resistance R_w . The probe consists of a cylindrical body equipped with two prongs onto which the wire is soldered. The probe is connected to an electrical source, which supplies a current of intensity I to the wire (Figure 4.11). The sensing element is placed in a stream in order to measure its temperature $T_g(t)$ varying with time.

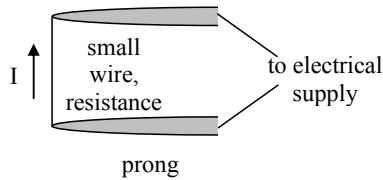


Figure 4.11. Cold-wire measurements. Sketch of the probe

The temperature T_w of the electric wire is measured via its electric resistance R_w , which is related to the temperature by

$$R_w = R_0 [1 + \beta_w (T_w - T_0)] \quad [4.28]$$

where R_0 is the wire resistance at the reference temperature T_0 and β_w , the temperature coefficient of the wire material.

Measurements are correct if the wire temperature is very close to that of the fluid (T_g) to be measured. Hence, the current intensity I ($I = \text{Constant}$) used to measure the resistance R_w must be very small. Typical values for a platinum wire are:

$$d = 1.5 \mu\text{m}, l = 1 \text{ mm}, R_0 = 100 \Omega, I = 0.3 \text{ mA}, \beta_w = 3.8 \cdot 10^{-3} \text{ K}^{-1}$$

$$\text{solid density } \rho_w = 21.5 \cdot 10^3 \text{ kg m}^{-3}, \text{ solid heat capacity } c_w = 133 \text{ J kg}^{-1} \text{ K}^{-1}$$

4.8.2. Guidelines

Estimate the difference $T_w - T_g$ in steady conditions, i.e. when the wire is placed in a stream of velocity U and temperature T_g , constant with time. We assume that heat losses by radiation and axial conduction to the prongs along the wire are negligible. Numerical application: air at 20°C , kinematic viscosity $\nu = 15 \times 10^{-6} \text{ m}^2 \text{ s}^{-1}$, $U = 15 \text{ m s}^{-1}$.

When the fluid temperature T_g fluctuates with time, the probe temperature also varies, but due to the thermal inertia of the wire, the measured signal is damped and shifted with respect to T_g . Evaluation of the response time of the probe is proposed. Write the equation giving the variations of T_w with time. Calculate the time constant of the probe as a function of velocity U and diameter d .

Calculate the damping and phase lag of T_w relative to T_g for a sinusoidal temperature signal T_g of frequency f . Numerical application: $f = 1 \text{ kHz}; 10 \text{ kHz}$.

4.8.3. Solution

4.8.3.1. Steady conditions

If heat losses are ignored, the electric power dissipated by Joule effect in the wire is balanced at thermal equilibrium by the rate of heat exchanged by the wire to the ambient fluid. This heat transfer rate corresponds to forced convection around the cylindrical wire.

The heat-generation rate due to Joule effect is $R_w I^2$.

The heat transfer rate between the cylindrical wire and the fluid is given by [4.6]

$$q_{conv} = \pi k (T_{w0} - T_{g0}) \overline{Nu}$$

where T_{w0} , T_{g0} denote the equilibrium temperature of the wire and the constant fluid temperature respectively. The Reynolds number is $Re = \frac{15 \times 10^{-6}}{15 \times 10^{-6}} = 1$.

The Collis and Williams law [4.8] gives $\overline{Nu} = 0.24 + 0.56 Re^{0.45} = 0.8$.

The equilibrium temperature is therefore

$$T_{w0} - T_{g0} = \frac{R_w I^2}{\pi k \overline{Nu}}$$

or $T_{w0} - T_{g0} = 0.14K$ with the conditions as given in section 4.8.1.

4.8.3.2. Unsteady conditions

When the fluid/wire temperatures fluctuate with time, the thermal budget of the wire yields

$$m c_w \frac{dT_w(t)}{dt} = R_w(t) I^2 - \pi k [T_w(t) - T_g(t)] \overline{Nu} \quad [4.29]$$

where m is the mass of the cylindrical wire $m = \rho_w \pi \frac{d^2}{4} l$.

At any instant there is a difference between the heat rate dissipated by Joule effect and the convective heat rate removed by the fluid. This difference is stored in or lost by the wire (left-hand side of equation [4.29]). We assume that the heat

transfer law of the steady regime is still available in the present situation. This assumption then gives $\overline{Nu} = 0.8$.

Introducing relation [4.28] between the resistance $R_w(t)$ and the fluid temperature $T_w(t)$, equation [4.29] yields:

$$mc_w \frac{dT_w(t)}{dt} = R_0 I^2 + \left(R_0 \beta_w I^2 - \pi l k \overline{Nu} \right) T_w(t) - R_0 \beta_w I^2 T_0 + \pi l k \overline{Nu} T_g(t) \quad [4.30]$$

This first-order equation shows that the wire temperature $T_w(t)$ follows the fluid temperature variations $T_g(t)$ with the time constant

$$M = \frac{mc_w}{\pi l k \overline{Nu} - R_0 \beta_w I^2} \approx \frac{mc_w}{\pi l k \overline{Nu}} \quad [4.31]$$

or, replacing the cylinder mass in favor of d

$$M \approx \frac{\rho_w c_w d^2}{4k \overline{Nu}} \quad [4.32]$$

The Nusselt number varies roughly as $Re^{1/2}$. Hence, the time constant varies as $1/\sqrt{U}$ and as $d^{3/2}$. It is therefore recommended to use a wire with a diameter as small as possible in order to reduce M .

For a velocity of 15 m s^{-1} and the data given above, equation [4.32] gives $M = 0.03 \text{ ms}$.

In order to characterize the probe response, we consider sinusoidal variations of the fluid temperature $T_g(t) - T_{g0} = a \cos \omega t$. The probe temperature also varies sinusoidally with a phase lag φ such that $T_w(t) - T_{w0} = b \cos(\omega t - \varphi)$.

Substituting into equation [4.30], we identify the terms in $\cos \omega t$ and $\sin \omega t$ to obtain the signal damping and phase lag:

$$\frac{b}{a} = \frac{1}{\sqrt{1 + M^2 \omega^2}} \quad [4.33]$$

$$\text{tg } \varphi = M \omega \quad [4.34]$$

With the data of the problem, we find for:

$$f = 1 \text{ kHz}, \quad b/a = 0.98, \quad \varphi = 10.7^\circ$$

$$f = 10 \text{ kHz}, \quad b/a = 0.47, \quad \varphi = 62^\circ$$

With a cold-wire of $1 \mu\text{m}$, it is then possible to measure temperature fluctuations of the order of 1 kHz. In order to perform measurements at higher frequency, a wire of smaller diameter must be used ($0.6 \mu\text{m}$).